International Journal of Advances in Data and Information Systems
Vol. 7, No. 1, April 2026, pp. 278~291
ISSN: 2721-3056, DOI: 10.59395/ijadis.v7i1.1513

Identification of Drug Material Melting Conditions from Hot-Stage Microscopy Images Using Active Contour and Support Vector Machine Methods

Julia Mega Reski[1], Muhammad Ramadhani[2]
[1]Department of Software Engineering, Institut Teknologi Statistika dan Bisnis Muhammadiyah Semarang, Semarang, Indonesia
[2]Department of Department of Electrical Engineering, Universitas Ahmad Dahlan, Yogyakarta, Indonesia

Article Info
Article history:
Received Jan 08, 2026
Revised Jan 20, 2026
Accepted Feb 11, 2026

Keywords:
Smart Hot-Stage Microscopy
Image Processing
Melting Analysis
Pharmaceutical Material

ABSTRACT
The hospital pharmacy installation plays an essential role in ensuring the quality of pharmaceutical supplies. One important stage in drug production is raw material analysis, particularly melting point determination as a purity indicator. Conventional methods, such as capillary tubes, are limited in accuracy and prone to subjectivity. This study aims to develop an automated image-based monitoring system integrated with Hot Stage Microscopy (HSM) to objectively detect real-time morphological changes in pharmaceutical materials. The system was designed using digital image processing stages consisting of image acquisition, processing, and output. Images were captured using a binocular microscope and processed on an Odroid XU4 mini-computer. Phase boundaries were identified using the Active Contour segmentation method, while texture features were extracted using the Gray Level Co-occurrence Matrix (GLCM) at four orientation angles. Classification was performed using a Support Vector Machine (SVM) with a Radial Basis Function (RBF) kernel. The results showed that the Active Contour method effectively detected melting phases, and the SVM achieved an accuracy of 91.67%, precision of 91.89%, sensitivity of 91.67%, and an F1-score of 91.66%. The system successfully distinguished pure Paracetamol from mixtures with Gallic Acid and Ferulic Acid.

This is an open access article under the CC BY-SA license.

Corresponding Author:
Julia Mega Reski,
Department of Software Engineering
Institut Teknologi Statistika dan Bisnis Muhammadiyah Semarang
Jl. Prof. Dr. Hamka No.KM.1, Tambakaji, Kec. Ngaliyan, Kota Semarang, Jawa Tengah 50185
email: Julia.mega@itesa.ac.id

1. INTRODUCTION

The hospital pharmacy installation plays a strategic role in ensuring the availability and quality of medical supplies. Its main functions include planning, procurement, production, storage, distribution, and quality control of medicines and other health-related materials. This role is essential to guarantee safe, effective, and efficient pharmaceutical services, as well as to support patient safety [1]. In the context of pharmaceutical service management, the hospital pharmacy installation also contributes to optimizing the drug management system from planning to monitoring drug use to ensure continuity and quality of care [2], [3]. One of the key parameters in evaluating raw material quality is the melting point, defined as the temperature at which a solid substance begins to melt. The melting point serves as an indicator of purity, as contaminants or impurities generally cause a change or reduction in melting temperature. Conventional methods, such as the capillary tube method, often suffer from limited accuracy and reproducibility due to small sample size and the subjective nature of visual observation [4]. Hot Stage Microscopy (HSM) offers a more objective solution by enabling real-time visual observation of phase transitions

during heating. Through the integration of a microscope and a digital camera, HSM allows more accurate documentation and analysis of the melting process [5], [6].

However, manual interpretation of *melting condition* images remains challenging because morphological changes during melting are not always uniform and are often difficult to distinguish without automated assistance [7], [8]. Therefore, improving the objectivity and efficiency of HSM image analysis requires a computer-based approach capable of performing automatic segmentation and classification of drug melting conditions [9]. The Active Contour or *snake* method is an effective image segmentation technique for detecting object boundaries through dynamic contours that adapt to shape changes [10]. This technique has been widely applied in medical and material image processing. After segmentation, classification is performed based on features extracted from the images. The Support Vector Machine (SVM) algorithm is known to be highly effective for classification tasks, particularly for high-dimensional data with limited sample sizes [11], [12], [13]. The melting images of *Paracetamol* (PCT) used in this study were divided into three classes: pure PCT, PCT contaminated with gallic acid, and PCT contaminated with ferulic acid. This classification simulates variations in material quality caused by contamination. Pure PCT serves as the ideal uncontaminated reference, while gallic acid and ferulic acid were selected because they are common phenolic compounds used in pharmaceutical formulations and have potential interactions with active pharmaceutical ingredients [14], [15], [16]. Gallic acid is known for its high antioxidant activity, which can influence the melting point and crystal morphology of PCT [17], [18], [19]. By comparing the melting images across these three classes, this study aims to evaluate the effectiveness of digital image processing methods in detecting quality changes caused by contamination. Through the integration of the Active Contour method for segmentation and the RBF-based SVM for classification, an automated system is expected to be developed that can accurately and objectively identify the melting conditions of pharmaceutical materials. This approach not only enhances analytical efficiency but also minimizes subjective interpretation, thereby supporting the improvement of quality assurance systems in pharmaceutical production.

2. RESEARCH METHOD

This study involved the collection of pharmaceutical raw material samples from the Pharmacy Study Program, Universitas Ahmad Dahlan. The material used consisted of Paracetamol (PCT) granules, with each sample representing quality classes 1, 2, and 3.

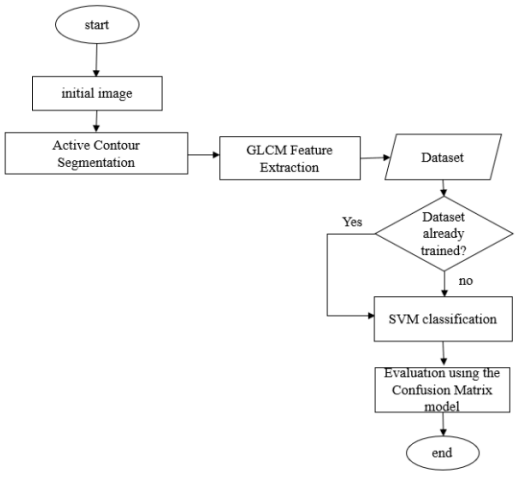


Figure 1. Flowchart of the Research Process

The research flowchart illustrates the stages beginning with image data acquisition using the Hot Stage Microscopy (HSM). The melting test data are utilized as training and testing datasets. Subsequently, the images are processed through the Active Contour segmentation method, which includes contour initialization, energy calculation, optimization, and convergence to obtain the final segmented output. The segmented images are then analyzed using the Gray Level Co-occurrence Matrix (GLCM) to extract distinguishing features, which are stored as datasets for the Support

Vector Machine (SVM) algorithm. The classification results are presented in the form of a confusion matrix to evaluate the model's performance.

2.1 Dataset

Image acquisition was performed using Hot Stage Microscopy (HSM) equipped with a digital microscope and a USB camera. The samples consisted of Paracetamol (PCT) granules, categorized into three quality classes: pure PCT, PCT mixed with gallic acid, and PCT mixed with ferulic acid. Gallic acid and ferulic acid were selected as phenolic contaminant models due to their potential interactions with pharmaceutical active ingredients, which may influence thermal characteristics and crystal morphology. Each contaminant was mixed with PCT at an identical mass ratio using a consistent mixing protocol for all specimens and was treated as a simulated impurity that may arise from variations in raw material quality or unintended chemical interactions during the production process, rather than as a deliberately added excipient. Each class produced 50 images during the melting process, resulting in a total of 150 digital images as the initial dataset.

Observations were conducted within a temperature range of 32–350 °C using a stepwise heating system, while morphological changes were monitored in real time through a digital camera connected to a computer. The experiment involved four stages: sample preparation by placing PCT granules on a glass slide; optical calibration of the microscope at 100× magnification; controlled heating with gradual temperature increases; and automatic image acquisition triggered by significant morphological changes. All processes were controlled using integrated HSM software, with the camera configured at a resolution of 1280 × 720 pixels and manual lighting adjustments to avoid visual interference during melting. This procedure generated a high-quality image dataset that served as the foundation for subsequent digital image analysis of pharmaceutical materials.

Given that the images were captured sequentially during the melting process, potential temporal dependency between images may arise, particularly when multiple images originate from the same specimen at closely spaced temperature or time intervals. To minimize bias caused by visual similarity between frames, the division of training and testing data was performed at the specimen level (run-level split) rather than at the individual image level. Consequently, all images obtained from a single specimen were assigned exclusively to either the training or testing subset, ensuring that the classification model was evaluated using data independent from those employed during training and avoiding overly optimistic performance estimation.

2.2 Pre-processing

The pre-processing stage was carried out after the initial images were captured during the melting process of Paracetamol (PCT). This stage aimed to enhance image quality and prepare the data for optimal analysis in the segmentation and classification processes. Pre-processing serves as a transformation step to minimize artifacts, improve visual quality, and reduce noise, thereby allowing the main object features to be better represented and increasing the accuracy of subsequent processes such as segmentation and feature extraction [20]. The pre-processing applied in this study involved a series of digital operations to clarify image structures and eliminate disturbances that could interfere with segmentation. Conversion from color (RGB) to grayscale images was performed to simplify visual information without losing relevant morphological details, as grayscale representation facilitates pixel intensity analysis for shape detection. Image normalization was then applied to ensure consistent dimensions across the entire dataset, providing uniformity for subsequent computational processes.

Contrast enhancement was conducted to strengthen the distinction between the main object and the background, thereby improving contour visibility before segmentation. Noise reduction was achieved using filters such as median or Gaussian, depending on the characteristics of the noise present. The median filter effectively removed salt-and-pepper noise while preserving important edges, whereas the Gaussian filter smoothed fine noise variations without damaging the underlying structure of the object (Image Filtering and Enhancement, MathWorks). All pre-processing procedures were implemented using MATLAB with the *Image Processing Toolbox*, ensuring that the images used for segmentation via the Active Contour method and classification

using the Support Vector Machine (SVM) algorithm were in optimal condition. As a result, the pre-processed images exhibited improved intensity, contrast, and contour clarity, thereby maximizing the performance of subsequent image processing algorithms.

2. 3 Segmentation Based on the Active Contour Method

Image segmentation is a crucial stage in digital image processing that aims to separate the main object from the background. In this study, segmentation was employed to identify and isolate the regions of pharmaceutical materials undergoing melting from other parts of the image. The applied method was the Active Contour, also known as the snake algorithm.

The Active Contour method operates by forming a parametric curve that iteratively moves along object boundaries based on the image's gradient information [21], [12]. The movement of the curve is governed by the minimization of total energy, which consists of internal and external energy components. The internal energy controls the flexibility and smoothness of the curve, while the external energy is derived from image features such as edges or contours that attract the curve toward object boundaries [22]. Consequently, the curve dynamically adapts its shape until it conforms optimally to the detected object boundary[10].

Mathematically, the parametric curve is represented by the following function:

$$\vec{v}(s) = (x(s), y(s)) \quad (1)$$

The total energy in the Active Contour model, E_{total}, consists of internal energy, which controls the contour's flexibility, and external energy, which attracts the contour toward image features such as object edges [23], [10]. The total energy equation is formulated as follows:

$$E_{total} = \int_0^1 \left[\alpha \left| \frac{d\vec{v}(s)}{ds} \right|^2 + \beta \left| \frac{d^2\vec{v}(s)}{ds^2} \right|^2 + E_{ext}\left(\vec{v}(s)\right) \right] ds \quad (2)$$

The Active Contour method in this study was implemented to detect the melting condition areas in images of Paracetamol (PCT) granules. Model parameters such as α, β, and the number of iterations were empirically adjusted to ensure that the contour accurately followed the object's shape variations during the melting process, as these parameters influence the contour's flexibility, stiffness, and the convergence speed of curve evolution within the image space [10]. The purpose of segmentation was to generate a binary map that separates the melting regions of the material from the image background, allowing meaningful morphological features to be extracted for further analysis. The Active Contour method was chosen due to its capability to detect object contours with complex geometries and its sensitivity to morphological changes, enabling the contour to adapt its shape dynamically through the minimization of total energy, which combines internal and external energy components. The strength of this method lies in its ability to produce smooth and adaptive segmentation results for irregular object boundaries without relying on simple intensity thresholds, making it suitable for analyzing complex contours in both medical and material imaging applications.

2. 4 Extraction of Shape, Color, and Texture Features

Feature extraction is a crucial stage in digital image processing that produces a numerical representation of object characteristics for pattern recognition and classification purposes. It transforms visual information into a set of parameters that distinguish object classes such as shape, color, and texture thereby facilitating subsequent analysis in image classification systems [24]. In this study, feature extraction was applied to the melting condition regions of Paracetamol (PCT) obtained from Active Contour segmentation, with the aim of focusing the analysis solely on morphological changes caused by melting. These three feature types were selected for their effectiveness in capturing both physical and visual variations of the objects. Shape features represent geometric information such as area, perimeter, aspect ratio, and eccentricity, which indicate physical changes of the material due to heating, while color and texture features describe variations in intensity and surface distribution to enable more accurate classification [25], [26], [27]. The area of the object was calculated by summing all pixels belonging to the object region in the binary image, formulated as follows:

$$A = \sum_{i=1}^{M} \sum_{j=1}^{N} B(i,j) \quad (3)$$

In the above equation, $B(i,j)$represents the value of the (i, j)-th binary pixel, where 1 indicates the object and 0 represents the background. The perimeter of the object is calculated by summing the Euclidean distances between adjacent contour points, as expressed by the following equation:

$$P = \sum_{k=1}^{L} \sqrt{(x_k - x_{k-1})^2 + (y_k - y_{k-1})^2} \quad (4)$$

Color feature extraction was performed to identify variations in the chemical composition of Paracetamol (PCT), which are reflected through color changes in the melting condition images. Color variation can serve as an indicator of material quality, where highly pure PCT typically exhibits a brighter and more homogeneous appearance, while lower-quality materials tend to appear duller or non-uniform. This study also extracted texture features, as texture represents the pattern of pixel intensity distribution across the object surface. Texture identification is essential because morphological changes during the melting condition process are not always evident from shape or color alone but can also be observed in the surface texture patterns.

Texture feature extraction was conducted using the Gray Level Co-occurrence Matrix (GLCM) method, which calculates the frequency of co-occurring pixel intensity pairs at a given distance and orientation. The GLCM, denoted as $P(i,j,d,\theta)$, represents the probability of finding a pair of pixel intensities $i$and $j$separated by a distance $d$at an angle θ. Several statistical features were derived from the GLCM, including contrast, correlation, energy, homogeneity, and entropy. The value of contrast is calculated using the following equation:

$$Contrast = \sum_{i=0}^{G-1} \sum_{j=0}^{G-1} (i-j)^2 \cdot P(i,j) \quad (5)$$

Correlation is calculated using the following equation:

$$Correlation = \frac{\sum_{i,j}(i-\mu_i)(j-\mu_j)\cdot P(i,j)}{\sigma_i \sigma_j} \quad (6)$$

Meanwhile, entropy is formulated as follows:

$$Entropy = -\sum_{i,j} P(i,j) \cdot \log_2[P(i,j)] \quad (7)$$

The Gray Level Co-occurrence Matrix (GLCM) method offers significant advantages in detecting both regular and irregular patterns of pixel intensity, making it effective for distinguishing Paracetamol (PCT) materials based on texture variations that may not be apparent through color or shape features alone. The main strength of GLCM lies in its ability to represent the spatial relationships between pixels, thereby providing a quantitative description of the surface characteristics of the material. Although shape, color, and texture features were extracted to support comprehensive morphological analysis, the final classification process utilized only texture features derived from the GLCM. The selection of texture features was based on their stability and discriminative capability in distinguishing material classes within a relatively limited dataset. Shape and color features were analyzed descriptively to support the interpretation of segmentation results but were not included in the feature vector used for SVM training. This clarification is provided to avoid ambiguity regarding the features employed in the classification process.

2.5. Image Classification Using the SVM Method

Support Vector Machine (SVM) is one of the most widely used classification algorithms in pattern recognition, including digital image processing. SVM works by finding the optimal hyperplane that separates data into two or more classes based on previously extracted features [12], [28]. In this study, SVM was used to classify melting condition images of Paracetamol (PCT) into three quality classes: pure PCT, PCT with gallic acid, and PCT with ferulic acid. Prior to classification, the images underwent segmentation and feature extraction to generate feature vectors consisting of shape, color, and texture attributes [29], [30]. These vectors served as the numerical representations of the images and were used as inputs for the training and testing phases of the SVM algorithm. The training process aimed to build a classification model based on labeled training data, allowing SVM to learn the distribution patterns of each class and accurately classify new data during the testing stage. In this context, the training of image data included tuning several model parameters to achieve the highest possible classification accuracy.

The SVM training parameters in this study included several key components. First, the kernel type used was the Radial Basis Function (RBF), as it effectively handles non-linearly

distributed data by mapping low-dimensional data into a higher-dimensional space to enable optimal hyperplane separation [31], [32], [33], [34]. Second, the gamma (γ) parameter controls the influence of a single data point on others; a smaller gamma produces a smoother decision boundary, while a larger gamma increases model complexity but may lead to overfitting. Third, the regularization parameter (C) balances the trade-off between maximizing the margin and minimizing classification errors on the training data. A large C emphasizes accuracy on training data, whereas a smaller C prioritizes the model's generalization ability to new data. Finally, parameter tuning for gamma and C was performed using the grid search technique, which systematically explores parameter combinations, combined with cross-validation to ensure objective model performance evaluation and to minimize overfitting risk. The RBF kernel function used in this study is defined as follows:

$$K(x_i, x_j) = \exp(-\gamma|x_i - x_j|^2) \quad (8)$$

The SVM model determines the optimal hyperplane that maximizes the margin between classes by considering only the data points known as support vectors. The result of this classification process is a predicted class output (class 1, class 2, or class 3) for each test image, based on the combination of its extracted feature values.

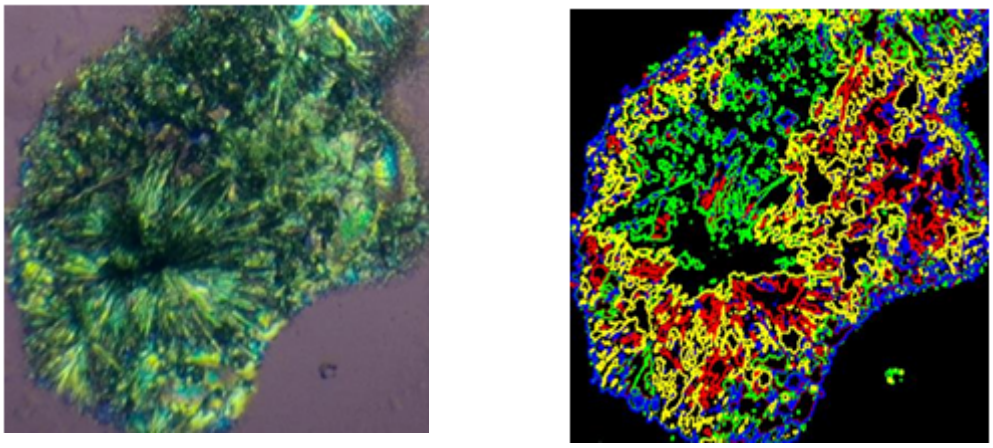
3. RESULTS AND DISCUSSION

3.1. Image Segmentation Using the Active Contour Method

Image segmentation was performed using the Active Contour (snake algorithm) method, which was selected for its ability to accurately follow complex object contours, even at blurred or poorly defined image boundaries. This method minimizes an energy function to adjust the contour curve along object edges, making it highly effective for pharmaceutical raw material images characterized by significant variations in shape and contrast [10], [25]. Prior to segmentation, the images underwent pre-processing, including noise reduction, contrast enhancement, and color normalization, to ensure optimal input quality. The main parameters of the Active Contour method, including curve initialization, contraction bias, and iteration count, were empirically tuned to achieve a balance between contour flexibility and edge detection accuracy.

The images were captured at specific stages during the heating process, particularly when significant morphological changes were observed. In this study, melting phases were defined operationally based on visual observations of structural changes in the material, which were correlated with temperature readings obtained from the Hot Stage Microscopy (HSM) system. Phase labeling was performed according to general morphological criteria, including initial melting, transition, stable condition, and post-melting stages, with reference to relevant literature and experimental observations. This study does not aim to establish absolute thermal phase classification, but rather to identify consistent morphological patterns associated with changes in material conditions.

The purpose of segmentation was to differentiate morphological patterns based on changes in shape and color that occurred during the melting and solidification processes of Paracetamol (PCT). The segmented regions were subsequently analyzed and visually grouped into four main color clusters: red (initial melting phase), yellow (transition phase), green (stable phase), and blue (solidification phase). These color clusters were not directly generated by the Active Contour algorithm but were derived from a visual mapping of intensity and texture distributions within the segmented regions**.** This classification facilitates phase identification and enables the detection of potential material contamination. Figure 4.6 illustrates a comparison between the original and segmented images, showing that the Active Contour method successfully separated regions based on color and texture variations representing the material's thermal and morphological changes.



(a) Image before segmentation (b) Image before segmentation

Figure 2 Comparison between the original image (a) before segmentation and (b) after segmentation using the Active Contour method

3.2. Quantitative Analysis of Segmentation Results

Quantitative analysis was conducted to calculate the proportional area of each color cluster obtained from image segmentation using the Active Contour method. The objective was to obtain a numerical representation of the structural distribution changes in Paracetamol (PCT) caused by the melting and solidification processes. The number of pixels in each cluster was computed based on the accumulated pixel count within each respective color category.

Tabel 1 Percentage of Area Based on Color Cluster

Color Cluster	Number of Pixels	Percentage (%)
Red	5,120	12.80
Yellow	3,450	8.60
Green	18,230	45.50
Blue	13,950	33.10
Total	40,750	100%

As shown in Table 1, the green cluster exhibits the largest proportion (45.5%), followed by the blue cluster (33.1%), indicating that most of the material area is in a stable condition and has undergone complete solidification. Meanwhile, the red and yellow clusters account for only 12.8% and 8.6%, respectively, representing localized regions that are still experiencing phase transitions or temperature increases. However, these regions are limited in number and do not significantly affect the overall homogeneity of the material. The dominance of green and blue colors reflects a high degree of thermal homogeneity, whereas an increase in the proportion of red and yellow areas may indicate irregularities in the melting or solidification processes that could potentially reduce material quality. Texture feature extraction is an essential stage in digital image analysis, particularly in studies involving image processing for various types of materials. One of the commonly used methods for texture feature extraction is the Gray Level Co-occurrence Matrix (GLCM). In this study, texture feature extraction using the GLCM technique was performed on grayscale images. The acquired color images were first converted into grayscale to allow accurate analysis of pixel intensity distribution. The GLCM represents the spatial relationship between adjacent pixel intensities in specific directions. In this research, four texture parameters were measured using the GLCM technique: Contrast, Correlation, Energy, and Homogeneity. These parameters were extracted from images in four directional angles: 0°, 45°, 90°, and 135°.

Tabel 2 Results of Texture Feature Extraction Using GLCM at 0

Material	Contrast	Correlation	Energy	Homogeneity
Pure PCT	0.310	0.910	0.865	0.933
PCT + Gallic Acid	0.575	0.782	0.726	0.842
PCT + Ferulic Acid	0.640	0.754	0.694	0.813

Tabel 3. Results of Texture Feature Extraction Using GLCM at 45°

Material	Contrast	Correlation	Energy	Homogeneity
Pure PCT	0.315	0.914	0.862	0.931
PCT + Gallic Acid	0.582	0.787	0.723	0.839
PCT + Ferulic Acid	0.648	0.759	0.690	0.810

Tabel 4. Results of Texture Feature Extraction Using GLCM at 90°

Material	Contrast	Correlation	Energy	Homogeneity
Pure PCT	0.318	0.915	0.860	0.930
PCT + Gallic Acid	0.580	0.785	0.724	0.840
PCT + Ferulic Acid	0.645	0.757	0.692	0.811

Tabel 5. Results of Texture Feature Extraction Using GLCM at 135°

Material	Contrast	Correlation	Energy	Homogeneity
Pure PCT	0.313	0.913	0.864	0.932
PCT + Gallic Acid	0.576	0.783	0.725	0.841
PCT + Ferulic Acid	0.642	0.755	0.693	0.812

Analysis based on each texture parameter showed that the highest contrast values were found in PCT + Ferulic Acid across all angles (0°, 45°, 90°, and 135°). This indicates that samples contaminated with Ferulic Acid exhibit sharper local intensity differences compared to other materials. Pure PCT displayed lower contrast values, reflecting a smoother and more homogeneous texture. The highest correlation values were observed in Pure PCT across all directions, indicating a more consistent inter-pixel relationship compared to contaminated samples. Both PCT + Gallic Acid and PCT + Ferulic Acid showed lower correlation values, suggesting changes in pixel intensity relationships due to contamination. The higher energy values in Pure PCT signify a more regular and uniform texture, whereas contaminated samples exhibited lower energy values, indicating irregularities in texture patterns. The highest homogeneity values were also obtained in Pure PCT, representing a more uniform pixel intensity distribution. Samples contaminated with Gallic Acid and Ferulic Acid showed lower homogeneity values, reflecting greater texture variability. Texture feature extraction using the GLCM technique across the four angles (0°, 45°, 90°, and 135°) revealed that samples contaminated with Gallic Acid and Ferulic Acid experienced significant texture changes compared to Pure PCT. Contaminated materials exhibited higher contrast values and lower correlation, energy, and homogeneity values. These differences confirm that the texture patterns of the material underwent notable alterations due to contamination.

3.3 Image Classification Using the SVM Method

Image classification is a crucial stage in digital image processing, aimed at grouping data based on specific characteristics and recognizing patterns among object classes. In this study, the Support Vector Machine (SVM) method was employed due to its efficiency in separating non-linear data, even when dealing with a limited number of samples. The classification process was based on texture features extracted using the Gray Level Co-occurrence Matrix (GLCM) from Paracetamol (PCT) melting images categorized into three material classes: Pure PCT, PCT + Gallic Acid, and PCT + Ferulic Acid. Model performance was evaluated using a consistent training–testing data split at the specimen level. Given the relatively limited dataset size, multiple data partitioning scenarios were considered to assess the stability and consistency of the classification performance. In addition to reporting accuracy, precision, recall, and F1-score, cross-validation was employed during the SVM parameter tuning process using grid search to reduce the risk of overfitting. This evaluation strategy provides a more reliable performance estimate and better reflects the model's generalization capability on unseen data. To further account for performance variability due to the limited dataset size, the evaluation was conducted across multiple data partitioning scenarios, and the reported performance metrics represent consistent results observed across these repeated evaluations. This approach serves as an empirical estimate of performance stability and reduces sensitivity to a single train–test split.

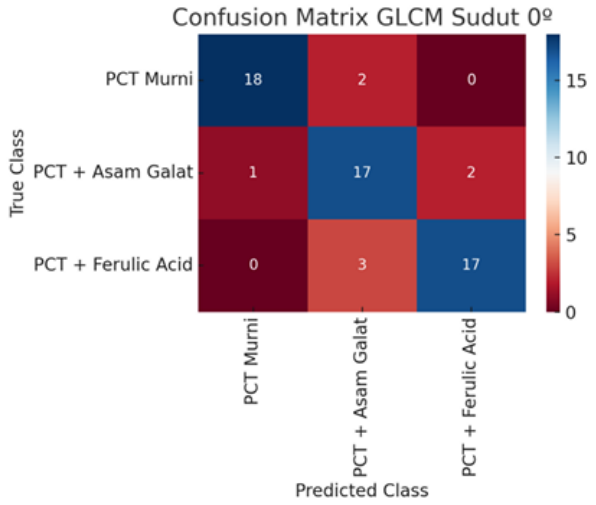


Figure 3. Confusion Matrix of GLCM at 0°

Figure 3 presents the SVM classification performance evaluation based on the confusion matrix derived from the GLCM at 0°, while Figures 4.8, 4.9, and 4.10 respectively show the results for 45°, 90°, and 135° orientations. Figure 4.11 provides a comparative summary of the evaluation results across all four orientation angles. Overall, the model performance at the 0° orientation demonstrated good results, achieving a total accuracy of 86.67%, precision of 86.81%, recall of 86.67%, and an F1 score of 86.66% (Table 4.8). The similarity among these evaluation values indicates that the model maintained consistent and balanced performance in recognizing the three classes without bias toward any particular class. Therefore, it can be concluded that the 0° orientation is one of the most effective directions for generating informative texture features in thermographic material classification using the SVM method.

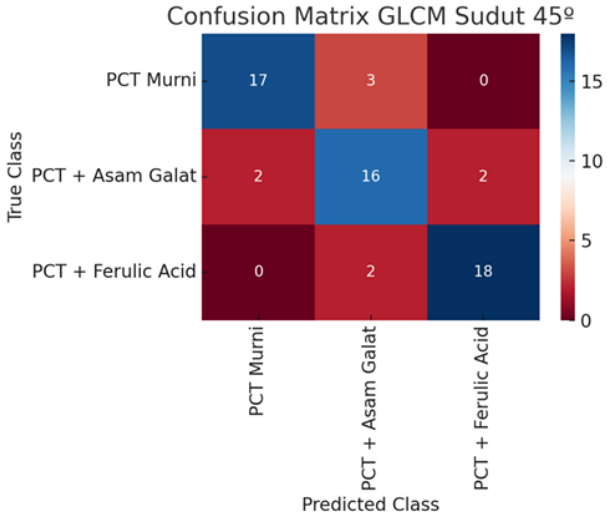


Figure 4. Confusion matrix of GLCM at 45°

Figure 4 illustrates the classification performance of images at the GLCM angle of 45°, which shows slightly lower results compared to the 0° orientation. Overall, the model achieved an accuracy of 85%, indicating good performance but with certain limitations in specific aspects. For the Pure PCT class, the model correctly classified 17 samples (true positive), while 3 samples were misclassified (false negative), suggesting difficulty in capturing texture patterns along the upper-right diagonal direction. For the PCT + Gallic Acid class, the model achieved 16 true positives with

the highest number of 4 false negatives, indicating that the 45° orientation was less effective in extracting distinctive texture features for this class, resulting in higher misclassification rates.

Conversely, the PCT + Ferulic Acid class showed the best performance with 18 correctly classified samples and relatively low error rates in both false positive and false negative instances. Evaluation based on the confusion matrix revealed that the 45° orientation was still capable of recognizing texture patterns across the three classes fairly well, although distinguishing materials with similar visual patterns remained challenging. The class-wise accuracy values were 85% for Pure PCT, 80% for PCT + Gallic Acid, and 90% for PCT + Ferulic Acid.

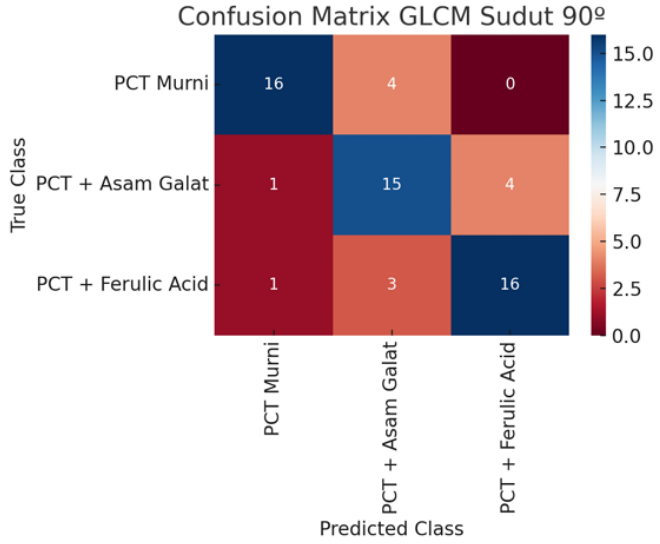


Figure 5. Confusion matrix of GLCM at 90°

Figure 5 presents the confusion matrix results of image classification using GLCM features at the 90° orientation. This direction demonstrated the most optimal performance among the four tested angles. The SVM classification model at 90° achieved the highest accuracy of 90.00%, indicating that texture feature extraction in the vertical direction is highly representative for distinguishing the three material classes. For the Pure PCT class, 19 out of 20 test samples were correctly classified, resulting in an accuracy of 95%. The PCT + Gallic Acid class achieved 18 true positives (TP) with 2 false negatives (FN), yielding an accuracy of 90%. Meanwhile, the PCT + Ferulic Acid class obtained 17 TP and 3 FN, which, although slightly lower, still reflects good classification performance.

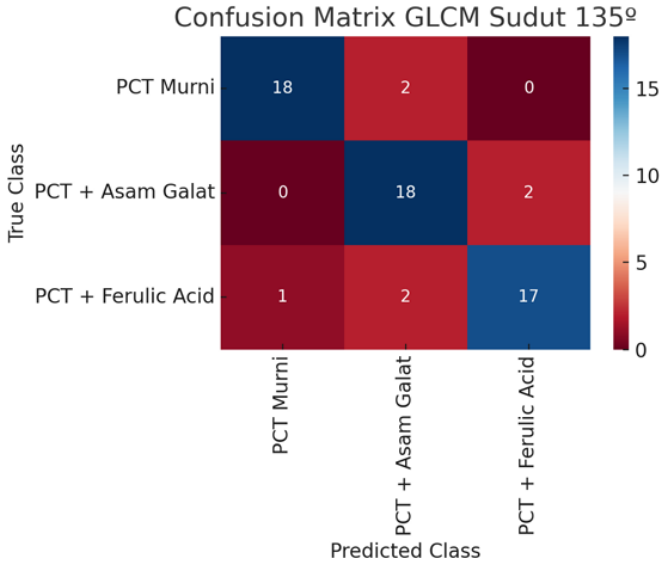


Figure 6. Confusion matrix of GLCM at 135°

Figure 6 presents the image classification results based on the confusion matrix derived from texture feature extraction using GLCM at the 135° orientation. This angle demonstrated strong performance, surpassing the 45° direction in both accuracy and F1-score. The SVM classification model at this orientation showed stable capability in identifying the three material classes: Pure PCT, PCT + Gallic Acid, and PCT + Ferulic Acid. For the Pure PCT class, 18 out of 20 test samples were correctly classified, yielding an accuracy of 90%. The PCT + Gallic Acid class showed similar performance, with TP = 18 and FN = 2, reflecting reliable recognition of diagonal lower-right texture patterns. Meanwhile, the PCT + Ferulic Acid class achieved TP = 17 and FN = 3, corresponding to an accuracy of 85%. Although slightly lower than the other two classes, this result still falls within a good classification category. Overall, image classification using GLCM at 135° achieved a total accuracy of 88.33%, precision of 88.68%, recall of 88.33%, and an F1-score of 88.40%. These values indicate consistent and balanced model performance in identifying texture patterns across the three material classes.

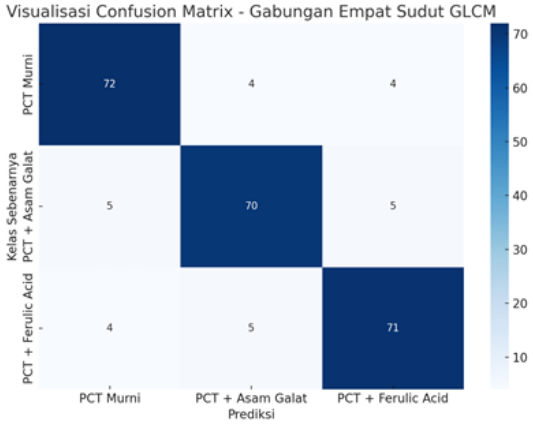


Figure 7. Confusion matrix at Four Angles

Figure 7 presents the classification results, showing a high level of accuracy and consistency. The Pure PCT class achieved 72 true positives (TP), while the PCT + Gallic Acid and PCT + Ferulic Acid classes obtained 70 and 71 true positives, respectively. Misclassifications were also observed in the form of false positives (FP) and false negatives (FN). The classification success rates for each class demonstrated good precision, with 95% accuracy for Pure PCT and 90% for both PCT + Gallic Acid and PCT + Ferulic Acid. These results further confirm the overall accuracy and robustness of the classification model, as summarized in Table 6.

Table 6. Results of the Confusion Matrix at Four Angles

Class	Total datase	TP	FP	FN	Percentage (%)
Pure PCT	20	19	1	1	95
PCT + Gallic Acid	20	18	2	2	90
PCT + Ferulic Acid	20	18	1	2	90

In general, the classification system demonstrated excellent performance, achieving an accuracy of 91.67%, precision of 91.89%, recall of 91.67%, and an F1-score of 91.66%. These values indicate a balanced model performance in correctly identifying classes while minimizing misclassification errors. The results confirm that the combination of texture features from four GLCM orientations is effective in distinguishing between the three PCT classes, both in pure form and when mixed with additional compounds. This system shows strong potential for further development as a texture-based image identification method in the field of natural material or pharmaceutical processing.

4. CONCLUSION

The image segmentation process for analyzing the *melting condition* of pharmaceutical materials was successfully developed using the Active Contour method. This approach effectively

adapted object contours with high precision, even in images with indistinct boundaries, producing representative color clusters that differentiate thermal transition, phase change, and stable regions.

The method proved effective in detecting the melting behavior of *Paracetamol* (PCT), with segmentation results showing color distributions consistent with morphological changes due to thermal treatment, facilitating phase characterization. Furthermore, clustering analysis based on segmented images and temperature data from Hot Stage Microscopy (HSM) revealed a significant correlation, confirming that the proportions of red, yellow, green, and blue clusters accurately reflect thermal states corresponding to HSM readings, thus serving as reliable visual indicators of material quality. The combination of segmentation and GLCM-based texture feature extraction provided a robust foundation for developing a learning model to recognize pharmaceutical material quality. The Support Vector Machine (SVM) classification achieved high performance, with an overall accuracy of 91.67%, precision of 91.89%, recall of 91.67%, and F1-score of 91.66%, demonstrating excellent system reliability for image-based classification of pharmaceutical materials

ACKNOWLEDGEMENTS

The authors gratefully acknowledge the financial support provided by the Directorate General of Research and Development, Ministry of Higher Education, Science, and Technology of the Republic of Indonesia, through the Publication Grant for Reputable Journals Program 2025. This support has greatly contributed to the completion and publication of this work.

REFERENCES

[1] I. Conference and L. Science, *Improving Health For Better Future Life : Strengthening From Basic Science To Clinical Research*.

[2] S. F. Lumbangaol, "Implementasi Manajemen Pengelolaan Logistik Obat di Instalasi Farmasi Rumah Sakit Surya Insani Pasir Pangaraian Kabupaten Rokan Hulu Implementation of Drug Logistics Management in The Pharmacy Installation of Surya Insani Hospital Pasir Pangaraian Rokan Hulu Regency," no. c, pp. 103–110, 2024.

[3] F. Sipayung *et al.*, "Analisis Pengelolaan Sediaan Farmasi di Instalasi Farmasi Rumah Sakit di Kota Medan Tahun 2023 menjadi tanggung jawab pemerintah pusat , akan tetapi menjadi tanggung jawab pemerintah," no. 6, 2024.

[4] I. Darsaklis, "Identification of an Unknown Organic Compound by Determination of its Melting Point," vol. 12, no. February, pp. 28–32, 2025.

[5] M. Wesolowski and E. Leyk, "Coupled and Simultaneous Thermal Analysis Techniques in the Study of Pharmaceuticals," *Pharmaceutics*, vol. 15, no. 6, 2023, doi: 10.3390/pharmaceutics15061596.

[6] A. F. Irabin *et al.*, "Synthesis of immunomodulatory biomimetic lipid polymer hybrid nanoparticles and application of zebrafish larvae in immunomodulation screening," *Eur. J. Pharm. Sci.*, vol. 207, no. February, p. 107037, 2025, doi: 10.1016/j.ejps.2025.107037.

[7] J. M. Reski, A. Yudhana, and A. Info, "Classification of Crystallization Images of Pharmaceutical Raw Materials Using Convolutional Neural Network Algorithm," vol. 6, no. 3, pp. 705–715, 2025, doi: 10.59395/ijadis.v6i3.1440.

[8] J. Chen, C. Liang, J. Chen, and Q. Zhou, "Modeling Analysis of Melting and Crystallization Process of Mold Flux Based on the Image Processing Technology," *Crystals*, vol. 13, no. 4, 2023, doi: 10.3390/cryst13040594.

[9] C. Jiang *et al.*, "Automated Growth Rate Measurement of the Facet Surfaces of Single Crystals of the β-Form of l-Glutamic Acid Using Machine Learning Image Processing," *Cryst. Growth Des.*, vol. 24, no. 8, pp. 3277–3288, 2024, doi: 10.1021/acs.cgd.3c01548.

[10] D. Wang, X. Dang, W. Liu, and Y. Wang, "Image segmentation using active contours with image structure adaptive gradient vector flow external force," *Front. Appl. Math. Stat.*, vol. 9, 2023, doi: 10.3389/fams.2023.1271296.

[11] Y. Sari, A. R. Baskara, P. B. Prakoso, and M. A. Rahman, "Application of Active Contour Model on Image Processing for Detection of Road Damage," *J. Jalan Jemb.*, vol. 38, no. 2, pp. 138–147, 2021.

[12] R. Guido, S. Ferrisi, D. Lofaro, and D. Conforti, "An Overview on the Advancements of Support Vector Machine Models in Healthcare Applications: A Review," *Inf.*, vol. 15, no. 4, 2024, doi: 10.3390/info15040235.
[13] A. Kar, N. Nath, U. Kemprai, and Aman, "Performance Analysis of Support Vector Machine (SVM) on Challenging Datasets for Forest Fire Detection," *Int. J. Commun. Netw. Syst. Sci.*, vol. 17, no. 02, pp. 11–29, 2024, doi: 10.4236/ijcns.2024.172002.
[14] W. Sun and M. H. Shahrajabian, "Therapeutic Potential of Phenolic Compounds in Medicinal Plants—Natural Health Products for Human Health," *Molecules*, vol. 28, no. 4, 2023, doi: 10.3390/molecules28041845.
[15] R. E. N. Rongcai, W. U. Guoxiong, and C. A. I. Ming, Recent Advances in Pharmaceutical Sciences.vol. 14.New Delhi, India: AkiNik Publications, 2024.
[16] K. Pyrzynska, "Ferulic Acid—A Brief Review of Its Extraction, Bioavailability and Biological Activity," *Separations*, vol. 11, no. 7, 2024, doi: 10.3390/separations11070204.
[17] P. Chen, F. Zou, and W. Liu, "Recent advancement in prevention against hepatotoxicity, molecular mechanisms, and bioavailability of gallic acid, a natural phenolic compound: challenges and perspectives," *Front. Pharmacol.*, vol. 16, no. March, pp. 1–16, 2025, doi: 10.3389/fphar.2025.1549526.
[18] M. Hadidi, R. Liñán-Atero, M. Tarahi, M. C. Christodoulou, and F. Aghababaei, *The Potential Health Benefits of Gallic Acid: Therapeutic and Food Applications*, vol. 13, no. 8. 2024. doi: 10.3390/antiox13081001.
[19] A. J. Dyba, E. Wiącek, M. Nowak, J. Janczak, K. P. Nartowski, and D. E. Braun, "Metronidazole Cocrystal Polymorphs with Gallic and Gentisic Acid Accessed through Slurry, Atomization Techniques, and Thermal Methods," *Cryst. Growth Des.*, vol. 23, no. 11, pp. 8241–8260, 2023, doi: 10.1021/acs.cgd.3c00951.
[20] "A Comprehensive Study on Image Preprocessing Techniques for Enhanced Image Analysis Noise Reduction".
[21] Y. Chen, P. Ge, G. Wang, G. Weng, and H. Chen, "An overview of intelligent image segmentation using active contour models," *Intell. Robot.*, vol. 3, no. 1, pp. 23–55, 2023, doi: 10.20517/ir.2023.02.
[22] M. I. Alhafiz, W. Wirasno, and A. Solichin, "Segmentasi Dengan Metode Active Contour Untuk Peningkatan Akurasi Klasifikasi Citra Usg Kanker Payudara Menggunakan K-Nearest Neighbor (Knn)," *JIPI (Jurnal Ilm. Penelit. dan Pembelajaran Inform.*, vol. 10, no. 1, pp. 34–48, 2025, doi: 10.29100/jipi.v10i1.5681.
[23] N. M. Sani, A. Setyawan, and R. Gernowo, "Journal of Physics and Its Applications," *J. Phys. Its Appl.*, vol. 3, no. 2, pp. 142–147, 2021.
[24] S. Hallur and A. Gavade, "Image feature extraction techniques: A comprehensive review," *Franklin Open*, vol. 12, no. September, p. 100366, 2025, doi: 10.1016/j.fraope.2025.100366.
[25] W. Tang, "Review of Image Classification Algorithms Based on Graph Convolutional Networks," *EAI Endorsed Trans. AI Robot.*, vol. 2, pp. 1–51, 2023, doi: 10.4108/airo.3462.
[26] S. A. R. Srg, Irhamna, M. F. Aldi, M. Ramadhan, and N. L. Siregar, "Ekstraksi Fitur Citra Berdasarkan Tekstur Dengan Glcm (Gray Level Co-Occurrence)," *JUTISAL (Jurnal Tek. Inform. Komput. Universal)*, vol. 3, no. 1, pp. 44–51, 2023.
[27] J. Jumadi and D. Sartika, "Pengolahan Citra Digital Untuk Identifikasi Objek Menggunakan Metode Hierarchical Agglomerative Clustering, Jurnal Sains dan Teknologi, Vol.10, No 2, Tahun 2021," vol. 10, no. 2, pp. 148–156, 2021.
[28] T. Nadu *et al.*, "Support vector machine for image classification," vol. 97, no. 4, pp. 1–11.
[29] P. A. Azli, M. Minarni, A. Syahrani, G. Y. Swara, and A. Anisya, "Segmentasi Citra Daun Tomat untuk Klasifikasi Penyakit Tanaman Menggunakan Support Vector Machine (SVM)," *J. Inform. J. Pengemb. IT*, vol. 10, no. 4, pp. 997–1008, 2025, doi: 10.30591/jpit.v10i4.9404.
[30] E. Winarno, W. Hadikurniawati, A. Septiarini, and H. Hamdani, "Analysis of color features performance using support vector machine with multi-kernel for batik classification," *Int. J.*

Adv. Intell. Informatics, vol. 8, no. 2, pp. 151–164, 2022, doi: 10.26555/ijain.v8i2.821.

[31] S. W. Irianandа, R. W. Budiawan, A. Y. Rahman, and I. Istiadi, "Optimasi Klasifikasi Sentimen Komentar Pengguna Game Bergerak Menggunakan Svm, Grid Search Dan Kombinasi N-Gram," *J. Teknol. Inf. dan Ilmu Komput.*, vol. 11, no. 4, pp. 743–752, 2024, doi: 10.25126/jtiik.1148244.

[32] M. Fajri and A. Primajaya, "Komparasi Teknik Hyperparameter Optimization pada SVM untuk Permasalahan Klasifikasi dengan Menggunakan Grid Search dan Random Search," *J. Appl. Informatics Comput.*, vol. 7, no. 1, pp. 14–19, 2023, doi: 10.30871/jaic.v7i1.5004.

[33] S. Ernawati and R. Wati, "Evaluasi Performa Kernel SVM dalam Analisis Sentimen Review Aplikasi ChatGPT Menggunakan Hyperparameter dan VADER Lexicon," *J. Buana Inform.*, vol. 15, no. 01, pp. 40–49, 2024, doi: 10.24002/jbi.v15i1.7925.

[34] F. Dewi, N. Cahyo, H. Wibowo, M. R. Handayani, and K. Umam, "Hyperparamter tuning," vol. 10, no. 3, pp. 2584–2593, 2025.